

EXPERIMENTAL AND ANALYTICAL VIBRATION CHARACTERISTICS OF AN RC PLANE MEMBER DAMAGED BY OUT-OF-PLANE SEISMIC LOADS

Seiji Nagata¹, and Toshimitsu Kanamitsu²

¹ Senior Research Scientist, Central Research Institute of Electric Power Industry, Chiba-ken, Japan
(n-seiji@criepi.denken.or.jp)

² Research Scientist, Central Research Institute of Electric Power Industry, Chiba-ken, Japan

ABSTRACT

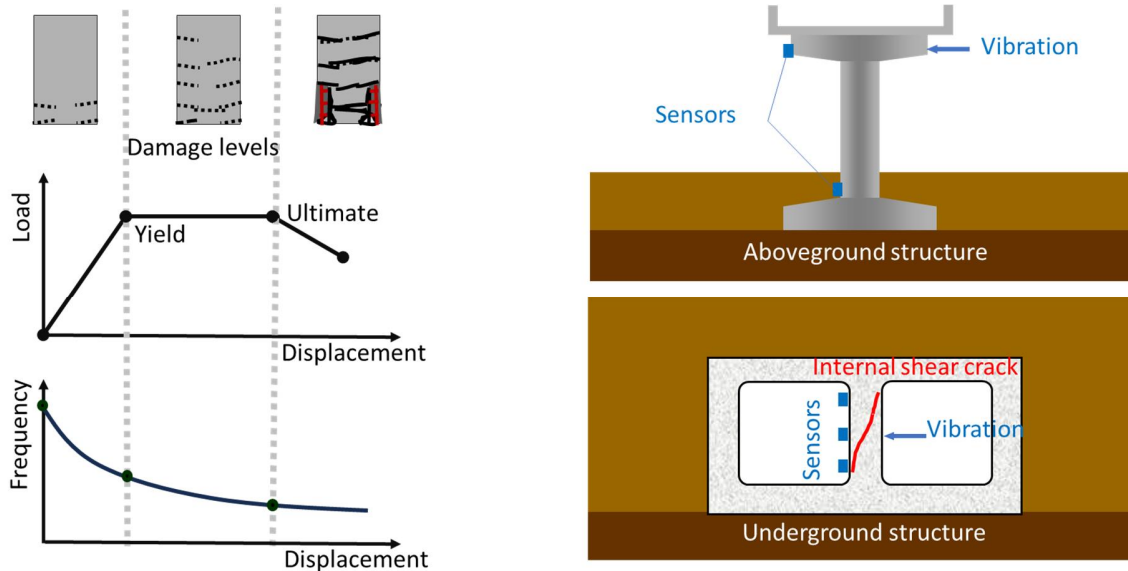
Changes in vibration characteristics of reinforced concrete (hereinafter, RC) structures can provide useful information for their damage assessment after a significant earthquake. This research involves a combination of static loading tests and forced vibration tests, as well as an analytical simulation using the finite element method, which has been conducted to evaluate the fundamental vibration characteristics of an RC member affected by the seismic damage. The test specimens were RC planar members without shear reinforcement, such that the progression of flexural and shear cracks can be observed. From the experimental results, in addition to a decrease in the fundamental natural frequencies, an increase in the number of resonance peaks which probably developed due to the occurrence of shear cracks was detected. On the other hand, it was shown that the decrease in the primary and secondary natural frequencies of the RC plane member can be well simulated based on the finite element model. However, more detailed modeling may be necessary to capture the increase in the number of resonance peaks.

INTRODUCTION

When RC civil engineering structures at nuclear power plants (JSCE 2021) damaged due to a significant earthquake, it is necessary to immediately assess the damage to make the restoration work smoothly. Damage after an earthquake is usually assessed by direct visual inspection, but damage is not always visible on the surface of structural members. In addition, it is difficult to assess the internal damage and the safety of the entire structure. As one of effective means of assessing the seismic damage to RC structures, there is a method that focuses on the change in the vibration characteristics of the structure (Rens et al. 1997; Aktan et al. 2000) as described figure 1. This method is particularly suitable for RC structures, since the natural frequency of RC structures changes as damage progresses (Neild et al. 2003; Seki et al. 2003; Nagata et al. 2012). This method has been mainly applied to aboveground structures such as bridges and buildings. In general, it is not considered to be suitable for underground structures where the influence of the surrounding ground is dominant. But the authors assume that it may be applicable when the vibration characteristics of individual members such as walls and floors are to be evaluated.

In order to obtain a basic knowledge on vibration characteristics at the component level, we have conducted vibration tests using a small vibration exciter on RC plane members subjected to out-of-plane loadings (Nagata and Kanemitsu 2024). Since analytical studies are also needed to show the certainty of the trends obtained in the vibration tests, in this paper, experimental as well as analytical natural vibration characteristics of the RC plane member are discussed. The test specimen is an RC plane member, which represents a wall or a slab in an RC under-ground structure. No shear reinforcing bars were used, to facilitate the examination of both flexural and shear cracks. In the static loading test, vertical loading and unloading corresponding to the out-of-plane direction were applied repeatedly. During the unloading phases of the static loading, forced vibration tests were conducted using a small exciter on the test specimen. A set of sweep excitations was induced on the specimen, and the resulting accelerations were measured to determine

the vibration characteristics of the RC plane member. In the simulation analysis, a static nonlinear analysis was firstly performed to simulate the dead load condition and the cyclic loading experiment. Then, the natural frequency and natural mode of the specimen were evaluated by performing an eigenvalue analysis using stiffness matrix that considers damage hystereses due to the static loads, to simulate natural vibration characteristics estimated from the vibration tests previously performed.



(a) Classification of damage levels of an RC member (b) Testing for above and underground structures

Figure 1. Outline of damage assessment for RC structures based on vibration testing.

TEST SPECIMEN AND EXPERIMENTAL CONDITIONS

Test Specimen

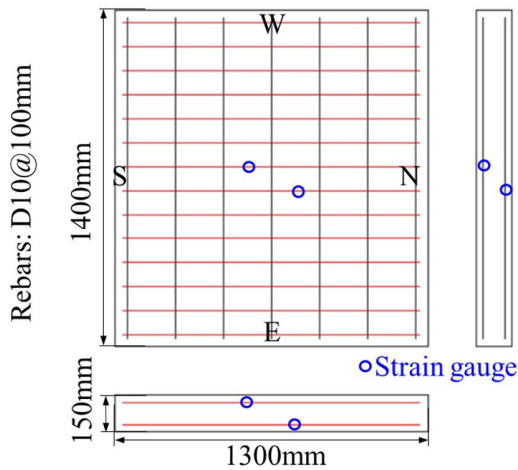
Figure 2 shows the geometry and the arrangement of reinforcing bars in the test specimen. It also shows the locations of strain gauges attached to measure the strain on the main reinforcing bars. The test specimen is an RC plane member with dimensions of 150 mm in thickness, 1,300 mm in length, and 1,400 mm in depth. The material and structural properties of the test specimen are detailed in Table 1. The design of these properties was guided by the Japanese guidelines and recommendations for the seismic performance verification of critical underground RC structures in nuclear power plants (JSCE 2021).

Main reinforcing bars of D10 (SD685) are arranged in a single row at both the top and bottom of the plane member with a cover thickness of 30 mm. The main reinforcement–bar ratio is 0.59%. No shear reinforcing bars were placed to allow for the examination of both flexural and shear cracks. The yield stress and Young’s modulus of the main reinforcing bars, as determined from tensile tests, were 761.2 MPa and 210.5 GPa, respectively. The compressive strength, tensile strength, and Young’s modulus of the concrete, assessed through cylinder tests on the day of testing, were 25.8 MPa, 2.08 MPa, and 26.3 GPa, respectively. The calculated flexural strength and shear strength of the specimen, based on existing formulas (AIJ 1999;

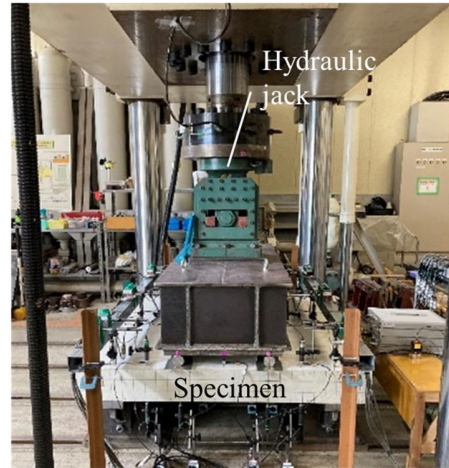
Niwa et al. 1986), were 348.7 kN and 520 kN, respectively. Consequently, the ratio of shear strength to flexural strength was estimated at 0.67%.

Table 1: Material and structural properties of the test specimen.

Property of concrete	Compressive strength	25.8 MPa
	Tensile strength	2.08 MPa
	Young's modulus	26.3 GPa
Property of longitudinal bars	Longitudinal-bar ratio	0.59%
	Diameter	10 mm
	Yield stress	761.2 MPa
	Young's modulus	210.5 GPa
Strength capacity of test specimen estimated from the material properties	Shear strength [8]	348.7 kN
	Flexural strength [9]	520.4 kN
	Strength ratio	0.67%



(a) Bar arrangement of the specimen

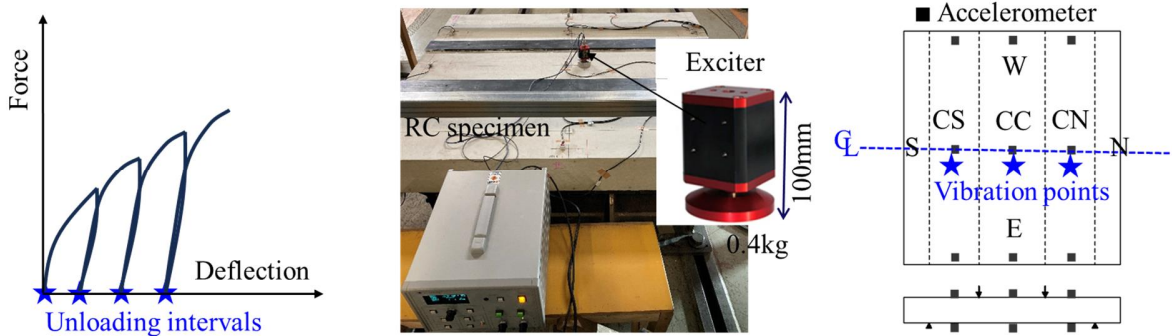


(b) Setup for the static loading test

Figure 2. RC test specimen and the loading setup.

Experimental Conditions

Figure 3 depicts the experimental setup used to induce seismic damage to the test specimen and the arrangement of displacement sensors. In this static loading test, the lower two lines of the RC plane member were simply supported, while loading and unloading in the vertical direction, corresponding to the out-of-plane direction of the RC plane member, were repeatedly applied through the upper two lines using a vertical jack. The vertical displacement was incrementally increased to achieve target drift angles (ratios of vertical displacement to shear span of the RC plane member) of 0.25%, 0.5%, 1.0%, and 2.0%. During the loading test, a vertical force was measured by the load cells installed in the vertical jack. Deflection of the RC plane member were also measured by displacement sensors positioned in the vertical direction. Strain gauges were attached to the main reinforcing bars on both the upper and lower sides of the member (see Figure 2) to measure the strain in these bars.



(a) Timing of the vibration test (b) Setup for the forced vibration test (c) Vibration and measuring points

Figure 3. Setups for the static loading test and the forced vibration test.

Figure 3 describes outline of forced vibration test (timing of vibration test, setting of small exciter and arrangement of accelerometer). The small exciter used here is S-0105 made by Asahi Seisakusho Ltd. Total length, weight, and excitation force of the exciter are approximately 100mm, 0.4 kg and 9.8 N respectively. In addition, frequency range, and maximum acceleration at no load are from 1 to 10kHz, and 245m/s², respectively. As for measurement, totally 18 strain accelerometers were attached on the top and bottom of the RC plane member. The measuring range of the acceleration, the sampling frequency, and the resolutions of the A/D conversions were 100m/s², 20 kHz, and 16 bits, respectively. The forced vibration test was conducted to the RC plane member in the vertical direction before loading and during unloading intervals of 0.5%, 1.0%, and 2.0% drift loadings, while removing the vertical jack. In the vibration testing, a set of sweep excitations was induced to the point CS, CC, and CN of the plane member (see Figure 6). The target acceleration of the sweep excitation was 40 m/s². While retaining the target acceleration, the frequency was changed from 50Hz to 700Hz over 45 seconds, to capture the fundamental natural mode shape as well as the natural frequency transition due to the seismic damage.

MODELING AND ANALYTICAL CONDITIONS

For simulation of the experimental behavior, a three-dimensional finite element analysis program DIANA 10.6 (DIANA FEA BV 2023) was applied. As constitutive laws of concrete, a total strain based orthogonal fixed crack model is applied. The constitutive model based on total strain was developed along the lines of the Modified Compression Field Theory, originally proposed by Vecchio and Collins (1986). Like the multi-directional fixed crack model, the total strain-based crack models follow a smeared approach for the fracture energy. The three-dimensional extension to this theory is proposed by Selby and Vecchio (1993). The analytical model for the RC specimen is depicted in Figure 4. The RC specimen is modelled with the nonlinear solid elements. The steel plate is modelled with linear solid elements. The total numbers of nodes and elements composing the concrete model are 18,126 and 14,560, respectively. The main reinforcements and the strength distribution reinforcements are modelled discretely as the embedded reinforcing bar elements assuming the complete bonding between the concrete and reinforcements.

Nonlinear stress-strain models presented in the Standard Specifications for Concrete Structures (JSCE 2023) was used for the stress-strain hysteresis in the compression side. For the tension nonlinearity, a tension softening model (Hordijk 1991) considering fracture energy based on the compression strength and the maximum aggregate size is used. Although the material parameters assumed in the model are basically determined based on the cylinder test results presented in Table 1, the tensile strength is set to 1.04 N/mm² equivalent to 50% of the test value. The Al-Mahaidi shear retention function (Al-Mahaidi 1979) was used to include the shear transfer behavior between the cracked surfaces of concrete, the compression strength

increment due to the lateral confinement of concrete is modeled based on the Hsieh-Ting-Chen failure surface (Hsieh et al. 1979). In the elements representing reinforcing bars, a bilinear stress-strain model, which considers the Von Mises yield criterion as well as the kinematic hardening effect, is applied. The material properties such as the Young's modulus and the yield strength are determined based on the tensile test results for the reinforcing bars described in Table 1. The secondary stiffness ratio to Young's modulus is set to 0.01 to provide the effect of strain hardening of these steel materials.

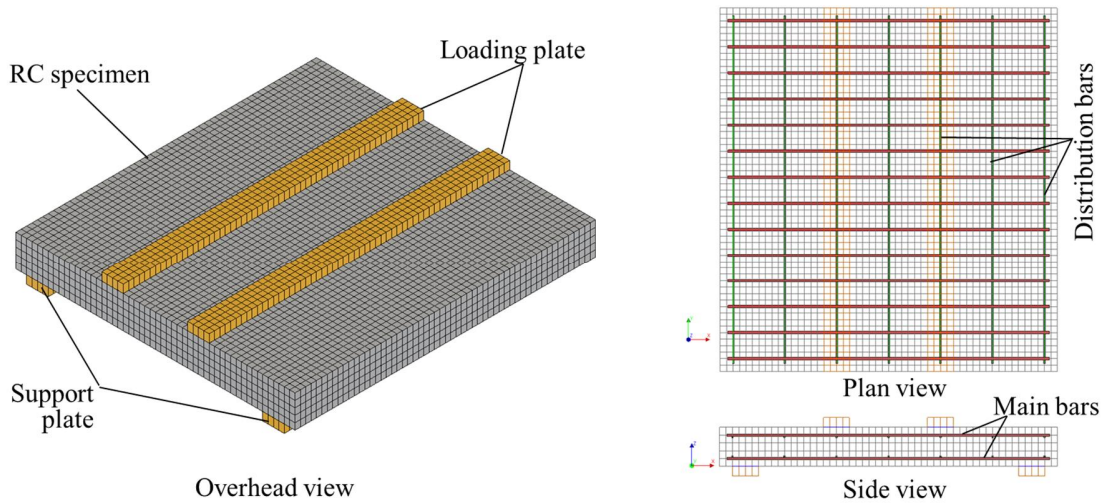


Figure 4. Three-dimensional nonlinear modeling for the analytical simulation.

As with the static loading test, the lower two support lines were fixed, and vertical displacement was repeatedly applied to the upper two loading lines in the nonlinear static analysis. Then, to simulate vibration tests performed during the unloading intervals, the static analysis was interrupted at the unloading point of the load-deflection hysteresis, and an eigenvalue analysis was performed while removing the displacement constrain at the upper two loading lines. Here, a function built into Diana 9.6 was applied to calculate the natural frequency and natural mode using the tangent stiffness matrix obtained by the nonlinear static analysis. In the following chapters, we will focus on the extent to which the damaged vibration characteristics from the vibration tests can be simulated by the combination of the nonlinear static analysis and the eigen value analysis.

COMPARISON OF EXPERIMENTAL AND ANALYTICAL RESULTS

Damage and Hysteretic Behavior

Before discussing the vibration characteristics, the hysteretic behaviours in the static loading test and the nonlinear static analysis are compared to understand the basic features of the damage patterns of the RC member. The vertical force versus deflection (drift angle) hystereses based on the experiment and the analysis are presented in Figure 5. As for the damage pattern, Figure 6 displays the damage on the E surface of the test specimen after the static loading test, where a shear crack is noted on the N side span. On the other hand, the contour plots of the maximum principal strain at the maximum displacement point and at its unloading point based on the nonlinear static analysis are presented in Figure 7. From these figures, the correlation between static experiments and analysis will be discussed as follows.

In the experiment, several flexural cracks occurred at the mid-span with a displacement of 0.1% drift loading, and a clear deterioration in stiffness was observed. Although a shear crack developed on the N side span of the E surface at a 1.5% drift loading, no significant decrease in the stiffness was noted. The strain of the main reinforcing bar has not reached the yield strain. The maximum crack widths of both flexural and shear cracks exceeded 0.5 mm, and the residual crack widths became narrow to 0.1 and 0.25 mm, respectively. This indicates that the shear crack tended to remain more easily than the flexural cracks after the unloading path.

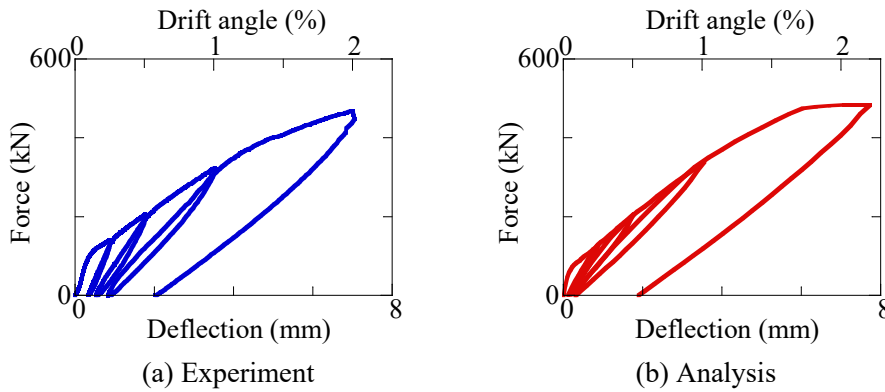


Figure 5. Comparison of the force versus deflection relationships.

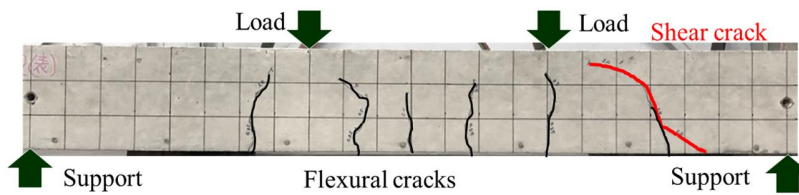


Figure 6. Damage of the test specimen after the static loading test (E surface).

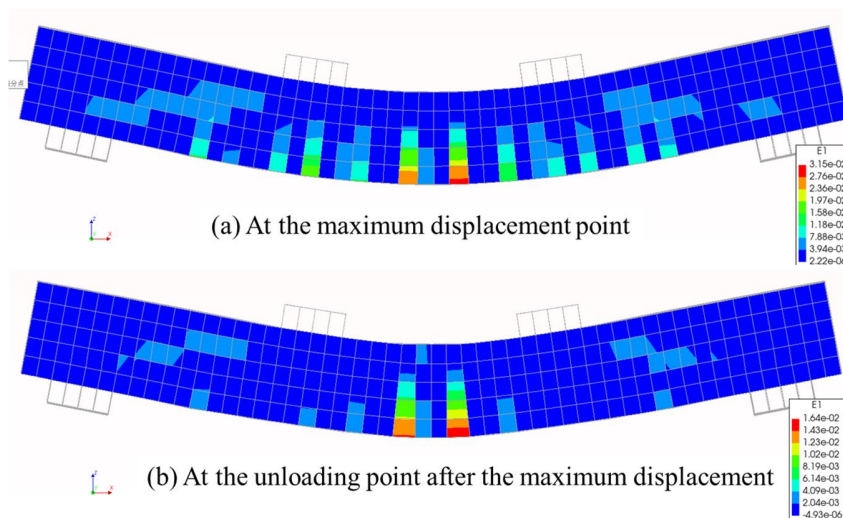


Figure 7. Contour plots of the maximum principal strain based on the nonlinear static analysis.

As mentioned above, the RC specimens exhibited nonlinear hysteresis mainly caused by cracking of the concrete, while the analytical model correlated well with such nonlinear hysteretic behavior, as shown in Figure 5. According to the contour diagram (see Figure 7), it is found that the maximum principal strain corresponding to the flexural cracks in the mid span and the shear cracks in the shear span caused by the load remain to a certain extent even after unloading. However, it is noted that the maximum principal strain corresponding to the flexural cracks is more significant than that corresponding to the shear crack, which is different from the tendency of the experiment.

Vibration Characteristics

To clarify the fundamental vibration characteristics of the RC plane member, the transfer functions were assessed based on the Fourier amplitude ratio derived from the accelerations measured at the concrete surface points CS, CC, and CN presented in Figure 3(c) and from the small exciter. Figure 8 and Figure 9 display the transfer functions of the RC member following the 1 % and 2 % drift loadings (corresponding to the timing before and after shear cracking, respectively), which have been obtained from the force vibration tests performed at the excitation point CS, CC, and CN. Based on the transfer functions of these two damage states, the difference in the vibration characteristics before and after the occurrence of shear cracking will be investigated as follows.

After the 1 % drift loading (see Figure 8), the spectra obtained by the three vibration tests (at the excitation point CS, CC, and CN) reveal resonance peaks at approximately 290 Hz that is consistent across the three measurement points (CS, CC, and CN). This value probably corresponds to the natural frequency of the first vibration mode (symmetric mode) of this RC plane member. Additionally, in measuring points CS and CN, resonance peaks with the same value were noted at approximately 450 Hz. This pattern may suggest that it corresponds to the natural frequency of the second vibration mode (anti-symmetric mode) of the RC plane member.

At meanwhile, according to Figure 9 (the results after the 2 % drift loading), a resonance peak at approximately 260 Hz is revealed in the three points of the spectra, corresponding to the first natural frequency for the symmetric mode. In the measuring points CS and CN, another resonance peak was noted at approximately 450 Hz. This may represent the natural frequency of the second vibration mode (anti-symmetric mode). Here, it is notable that after 1% drift loading, each resonance peak was clear, but after 2% drift loading (after shear cracks occurred), they became unclear. Moreover, at the experienced drift of 2%, an increase in the number of resonance peaks was noted, for example, at approximately 300 Hz at the measuring point CN. This tendency indicates that the occurrence of a shear crack may lead to an increase in the resonance peak.

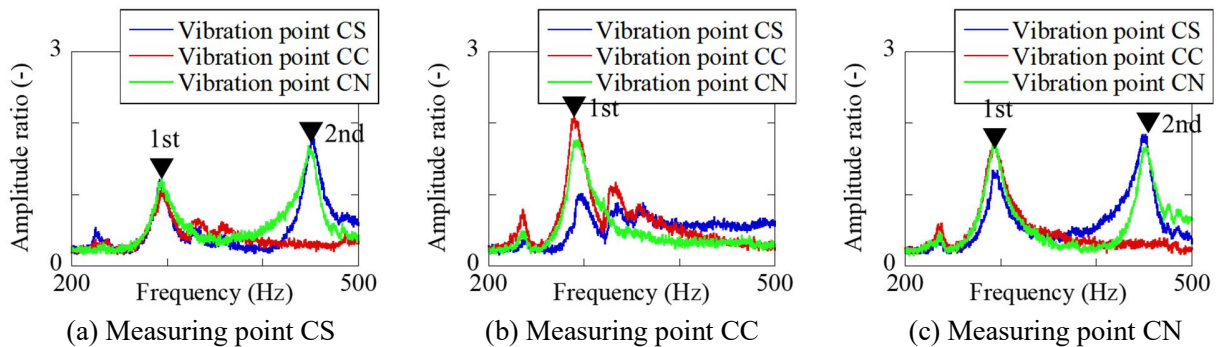


Figure 8. Transfer functions after 1.0% drift loading by the vibration test at the point CS, CC and CN.

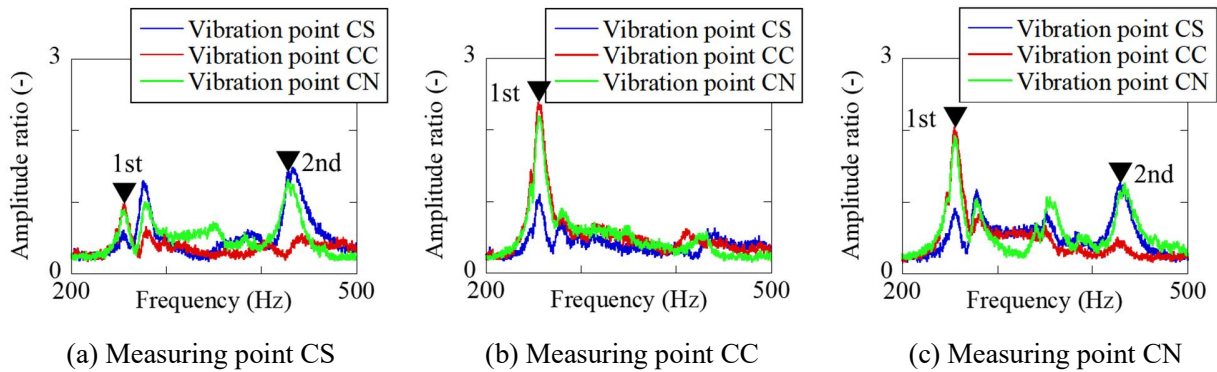


Figure 9. Transfer functions after 2.0% drift loading by the vibration test at the point CS, CC and CN.

Transition of the first and second natural frequencies of the RC plane member based on the experiment and the analysis are summarised in Figure 10. The experimental natural frequencies of their experienced drift angle in the experiment were estimated from the resonance peak of the transfer functions on the test specimen. On the other hand, the analytical natural frequencies were obtained from eigenvalue analysis performed at the unloading points at each drift angle in the nonlinear static analysis. From the observed transitions in resonance frequencies, decreases in both the first and second natural frequencies were confirmed, and this tendency can be well simulated based on the eigen value analysis considering the damage hysteresis.

Figure 11 presents the analytical natural mode shapes at the unloading point after the 2 % drift angle (unloading point). According to the calculated mode shapes, the first mode is a symmetrical mode with a natural frequency of 242 Hz, while the second mode is an inverse symmetrical mode with a natural frequency of 394 Hz. These characteristics generally align with the natural modes and frequencies estimated from the vibration tests, thereby demonstrating their validity. However, the analysis results showed that peculiar mode shape, in which local deformation was predominant, could not be observed. When trying to simulate the change in vibration mode due to shear cracks, it is considered to be difficult to do so with a distributed crack model in which cracks are uniformly distributed within the concrete element. It is considered that some ingenuity such as finer meshing will be necessary.

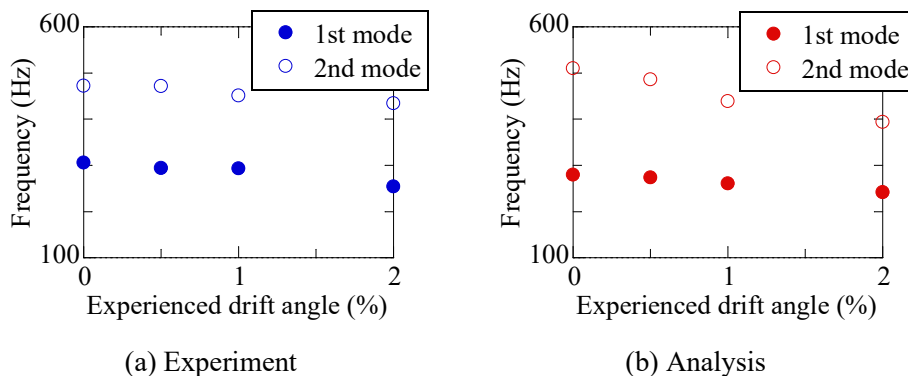


Figure 10. Transition of the fundamental natural frequencies based on the experiment and the analysis.

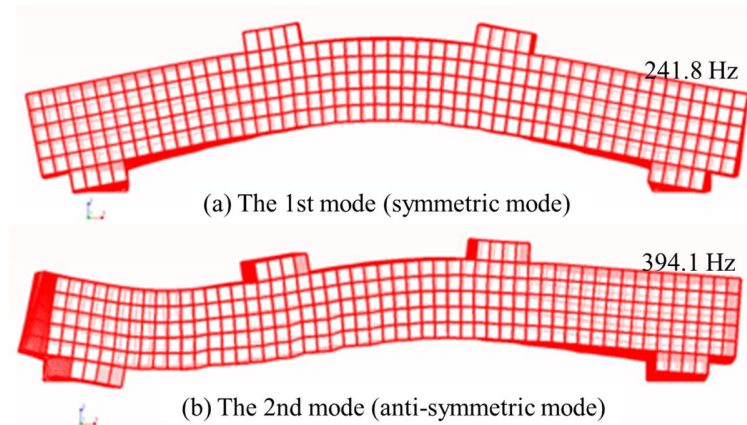


Figure 11. Analytical natural mode shapes at the unloading point after the maximum displacement.

CONCLUSIONS

In this study, a combination of the static loading test and the forced vibration test using a small exciter, as well as an analytical simulation using the three-dimensional nonlinear finite element method were carried out, to investigate the fundamental vibration characteristics of a damaged RC plane member. Several key findings related to the damage assessment of an RC structural member following a significant earthquake are obtained as follows.

- A series of experimental results indicated that a typical change observed in the vibration characteristics due to this loading hysteresis was a decrease in the fundamental natural frequencies. Additionally, an increase in the number of resonance peaks in the higher frequency region of the transfer function was detected. This suggests that local vibration modes of the RC member might emerge probably due to the development of a shear crack.
- It was demonstrated that the decrease in the primary and secondary natural frequencies of the RC plane member associated with the damage can be well simulated, based on the eigen value analysis considering the damage hysteresis. On the other hand, from this analysis results, the natural mode shape, in which local deformation was predominant, could not be observed.

Here, the authors present their conclusions from only one set of the experiment and the analysis. It is noted that further detailed investigations using more experimental and analytical cases on the natural modes considering seismic damage are required. Particularly, more detailed modeling must be necessary to capture and explain the emergence of the local vibration modes which may be associated with the occurrence of a shear crack.

ACKNOWLEDGEMENTS

The authors would like to express their sincere appreciations to Mr. H. Ohtsuka of the Shikakura Kikaku Corporation for conducting the static loading testing presented herein. Their appreciations also extend to Dr. G. Kou of the JIP Techno Science Corporation for his invaluable contributions in computing work using the finite element analysis program DIANA 10.6.

REFERENCES

- Aktan, A. E., Catbas, F. N., Grimmelsman, K. A. and Tsikos, C. J. (2000). "Issues in infrastructure health monitoring for management," *J. Engineering Mechanics*, ASCE, 126 (7), 711-724.
- Al-Mahaidi, R. S. H. (1979). *Nonlinear Finite Element Analysis of Reinforced Concrete Deep Members*, dept. Structural Engineering, Cornell University, Report No.79-1.
- Architectural Institute of Japan (1999). *Design Guidelines for Earthquake Resistant Reinforced Concrete Buildings Based on Inelastic Displacement Concept*, AIJ. (in Japanese)
- DIANA FEA BV (2023). *DIANA 10.6 User's Manual*.
- Hordijk, D. A. (1991). *Local Approach to Fatigue of Concrete*, PhD thesis, Delft University of Technology.
- Hsieh, S., Chen, W. F. and Ting, E. C. (1979). "An Elastic-fracture Model for Concrete," *Proc. Third Engineering Mechanics*, ASCE, 437-440.
- Japan Society of Civil Engineering (2021). *Expansion Version of Guidelines and Recommendations for Seismic Performance Verification of Critical Underground Reinforced Concrete Structures in Nuclear Power Plants*. Nuclear Power Civil Engineering Committee, JSCE.
- Japan Society of Civil Engineers (2023), Standard Specifications for Concrete Structures-2022 'Design'. (in Japanese)
- Nagata, S., Miyagawa Y., and Kanazawa, K. (2012). "Reduction of Natural Frequency due to Flexural Cracks or Shear Cracks in Reinforced Concrete Members," *Proc. the 15th World Conference on Earthquake Engineering*. 5609-5616.
- Nagata, S. and Kanemitsu, T. (2024). "Vibration-Based Damage Detection in a Reinforced Concrete Plane Member Using a Small Exciter," *Proc. the fib Symposium 2024, Zealand*, 2049-2056.
- Neild, S.A., Williams, M.S. and McFadden, P.D. (2003). "Nonlinear vibration characteristics of damaged concrete beams," *J. Structural Engineering*, ASCE, 129 (2), 260-268.
- Niwa, J., Yamada, K., Yokozawa, K. and Okamura, H. (1986). "Re-evaluation of the equation for shear strength of reinforced concrete beams without web reinforcement," *J. Structural Engineering/Earthquake Engineering*, JSCE, 372/V-5, 167-176 (in Japanese).
- Rens, K. L., Wipf, T. J. and Klaiber, F. W. (1997). "Review of non-destructive evaluation technique of civil infrastructure," *J. Performance Constructed Facilities*, ASCE, 11(4), 152-160.
- Seki, M., Nishimura, A., Sano, H. and Nakano, S. (2003). "Study on the evaluation of damage levels of RC rigid frame railway bridges in the case of earthquake," *J. Structural Engineering/Earthquake Engineering*, JSCE, 731/I-63, 51-64 (in Japanese).
- Selby, R. G., and Vecchio, F. J. (1993). *Three-dimensional Constitutive Relations for Reinforced Concrete*, Tech. Rep. 93-02, Univ. Toronto, dept. Civil Engineering, Toronto, Canada.
- Vecchio, F. J. and Collins, M. P. (1986). "The Modified Compression Field Theory for Reinforced Concrete Elements subjected to Shear," *ACI Journal* 83, 22, 219-231.